A new hand exoskeleton device for rehabilitation using a three-layered sliding spring mechanism

Arata, Jumpei
Department of Computer Science and Engineering, Graduate School of Engineering, Nagoya Institute of Technology

Ohmoto, Keiichi
Department of Computer Science and Engineering, Graduate School of Engineering, Nagoya Institute of Technology

Gassert, Roger
Rehabilitation Engineering Laboratory, Institute of Robotics and Intelligent Systems, ETH Zurich

Lambercy, Olivier
Rehabilitation Engineering Laboratory, Institute of Robotics and Intelligent Systems, ETH Zurich

他

出版情報：2013-10-17. Institute of Electrical and Electronics Engineers
バージョン：

A new hand exoskeleton device for rehabilitation using a three-layered sliding spring mechanism

Jumpei Arata[1], Keiichi Ohmoto[1], Roger Gassert[2], Olivier Lambercy[2], Hideo Fujimoto[1] and Ikuo Wada[3]

Abstract— **In this paper, a new hand exoskeleton device using a three-layered sliding spring mechanism is presented. In contrast to state of the art hand exoskeleton mechanisms (typically link, wire or pneumatically driven), the proposed mechanism is driven through large deformations of the compliant mechanism body. The mechanism can be made compact and lightweight by adequately positioning the compliant elements. In addition, the mechanism is designed to distribute 1-DOF actuated linear motion into three rotational motions of the finger joints, which translate into natural finger flexion/extension. The primary applicatoin of the proposed mechanism is to provide robotic support during physical therapy at the hospital (e.g. Continuous Passive Motion). However, thanks to its light and wearable structure, the proposed device could also be used at home as an assistive/therapeutic device to support activities of daily living. We introduce the mechanical structure of the three-layered sliding spring mechanism, present a prototype implementation as a hand exoskeleton device, and provide a preliminary evaluation.**

I. Introduction

In recent years, robotic technology has been adapted for physical rehabilitation in order to provide improved therapy and quantitative assessments of recovery [1]-[3]. In the area of robot-assisted rehabilitation, various robotic devices have been presented for the upper and lower extremities, mainly focusing on acute and chronic stroke survivors. While impairment of hand function is reported to be one of the most common problems after stroke[1],[4], designing robotic devices to treat and assist hand movements is a challenging task due to the complexity and versatility of the human hand. In past studies, two main approaches have mainly been taken: end-effector based [5] and exoskeleton [6]. End-effector based devices are mechanically grounded; thus, the size and weight are relatively unrestricted compared with exoskeleton devices. However, it is usually not possible to control each joint involved in the motion using end-effector based devices. An exoskeleton is generally a mechanism that can be placed around a part of the human body to mechanically guide or actuate it without impeding the joint's natural motion. For hand rehabilitation devices involving finger motion, the exoskeleton approach has mainly been taken to fit to the relatively small and complex structures of the hand, compared with the arms and lower limbs. However, designing hand exoskeleton devices is a challenging task due to the complexity and versatility of the human hand. Fitting the mechanical rotation center to the human joints (typically by using a remote center of motion, RCM) is one such problem to be addressed. In addition, hand exoskeleton devices typically involve a serially connected mechanical chain to transmit the motion to the distal part; thus, the mechanisms inherently suffer from large size, weight, and number of degrees of freedom (DOF), high mechanical complexity, and are often bulky and difficult to adapt to different subjects.

Hand exoskeleton devices in past studies have been developed mainly using link, wire or pneumatically driven mechanisms. Link mechanisms have been widely adapted since the early period of this area of research [6]-[9]. One of the most advantages of the link mechanisms is the robustness of power transmission (e.g. link can transmit bi-directional force unlike wire mechanisms). However, link mechanism inherently suffers from the size, weight, and backlash and play in mechanical linkage. Wire mechanisms are also typically employed to avoid complicated mechanical setups of serial chains in hand exoskeletons [10]-[15]. Wire mechanisms provide an ideal design solution for the size requirement to be reasonably fitted to the hand. However, as the wire only transmits the force uni-directionally, the mechanism becomes inherently complex to transmit bi-directional movements. In addition, wire extension and cut problems due to the transmitting force have to be taken into account for the design and control. Pneumatically driven mechanisms are typically chosen as an alternative approach [16]-[18]. In these mechanisms, pneumatic actuators are directly integrated (e.g. in a glove), thus the devices can be made compact and simple structure. However, precise guidance and assistance to the human joint centers are generally difficult, since the mechanical constraints are relatively limited in the direct integration approach using pneumatic actuators. Therefore, the pneumatically driven mechanisms have been mainly introduced to the devices with a relatively low number of DOFs without pricise joint center guidance/actuation.

From this background, we developed a new robotic device for hand rehabilitation based on a compliant mechanism. In such a mechanism, one or more elastic structures deform to transmit or transform the power in place of a conventional revolute joint [19]-[20]. The advantages of compliant mechanisms are: no backlash, no lubrication required, freedom

*This work was in part supported by A-STEP (AS232Z01775F), JST, Japan and the National Center of Competence in Research on Neural Plasticity and Repair of the Swiss National Science Foundation.

[1]J. Arata and K. Ohmoto and H. Fujimoto are with Department of Computer Science and Engineering, Graduate School of Engineering, Nagoya Institute of Technology, Gokiso-cho, Showa-ku, Nagoya 466-8555, Japan. jumpei at nitech.ac.jp

[2]R. Gassert and O. Lambercy are with the Rehabilitation Engineering Laboratory, Institute of Robotics and Intelligent Systems, ETH Zurich, 8092 Zurich, Switzerland.

[3]I. Wada is with Department of Rehabilitation, Nagoya City University Hospital, 1-Kawasumi, MIzuho-cho, Mizuho-ku, Nagoya 467-8602, Japan.

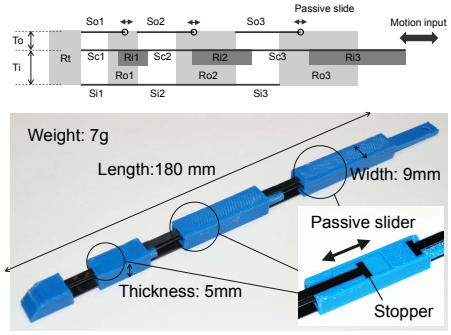

Fig. 1. Overview of the three-layered sliding spring mechanism.

from machine noise and abrasion powder, and most importantly, the mechanism can be made compact and lightweight thanks to the monolithic structure. In this paper, we propose a new multi-layered compliant mechanism to effectively incorporate the compliant mechanism into a robotic hand rehabilitation device. The proposed mechanism can be driven by a large deformation of the mechanism body; therefore, the mechanism can be compact and lightweight by adequately positioning the compliant elements. In addition, the mechanism is designed to distribute 1-DOF actuated linear motion into three rotational motions of the finger joints, distal interphalangeal joint (DIP), proximal interphalangeal joint (PIP) and metacarpophalangeal joint (MCP) to realize a natural finger bending (flexion/extension) motion, following the concept of a series elastic actuator. The primary application of the proposed mechanism is to provide robotic support during physical therapy at the hospital (e.g. Continuous Passive Motion). However, thanks to its light and wearable structure, the proposed device could also be used at home as an assistive/therapeutic device to support activities of daily living (ADL).

II. Three-layered sliding spring mechanism

To realize a compact and lightweight hand exoskeleton device, the following points were taken into account in the design concept: First, we focus on finger flexion/extension motion, to realize a robust hand grasping motion. Thus the 3 DOF flexion/extension motions are required on each finger module, however, the thumb can be fixed for the sake of robust grasping. Second, a finger module must be equipped with a RCM that is serially connected in the mechanical chain of 3 DOF flexion/extension. We then apply a compliant mechanism to address this issue. As a compliant mechanism is inherently soft compared to conventional mechanisms, the mechanism can be expected safe and highly adaptable to environment. Last, we limit the number of actuator as 1 DOF to reduce the mass and size, also for the sake of simplicity of the system. Thus the 3 DOF flexion/extension motions must be generated by a single actuator. This mechanical setup is an under-actuated mechanism, that is a mechanical system with fewer control inputs than the mechanism's DOF. In addition, the four fingers can be actuated simultaneously by a single actuator, by locating these four finger modules side by side, in a biomechanically correct setup. This setup

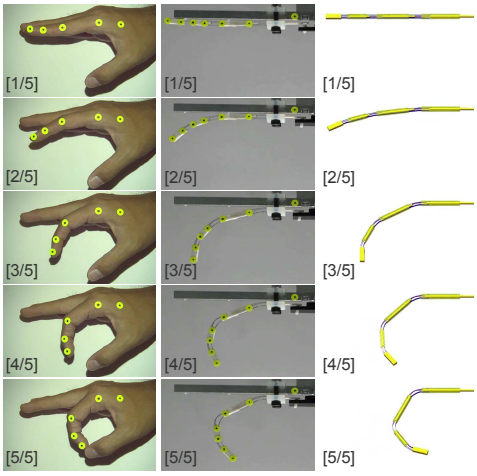

Fig. 2. Time series of pictures of the bending motion of the human index finger (left), the prototype mechanism motion (center), and FEM analysis results (right).

limits the performable motion, such as independent motions between fingers. However, the 1 DOF configuration largely contributes to the simplicity of the system.

A. Mechanism structure

An overview of the developed three-layered sliding spring mechanism is presented in Fig.1. The mechanism consists of three-layered sliding springs (inner, center, and outer springs as *Si*, *Sc*, and *So*, respectively) and rigid bodies (tip, inner, and outer parts as *Rt*, *Ri*, and *Ro*, respectively). The inner spring (*Si*) is located on the bottom of the mechanism and is fixed to the rigid bodies *Rt* and *Ro*; therefore, the spring blades Si_1, Si_2, and Si_3 that are connected to the rigid bodies at each end, simply function as flat springs. The spring blades Si_1, Si_2, and Si_3 are connected between *Rt* and Ro_1, Ro_1 and Ro_2, and Ro_2 and Ro_3, respectively. The center spring (*Sc*) is guided through a slit in the outer rigid bodies (*Ro*). Three inner rigid bodies (*Ri*) are separately fixed to the center spring; therefore, the connecting spring blades Sc_1, Sc_2, and Sc_3 between *Rt* and Ri_1, Ri_1 and Ri_2, and Ri_2 and Ri_3, respectively, function as independent springs. The outer spring (*So*) consists of three spring blades, So_1, So_2, and So_3, which are connected between the outer rigid bodies *Rt* and Ro_1, Ro_1 and Ro_2, and Ro_2 and Ro_3, respectively. Each proximal end of *So* is equipped with a passive slider mechanism and a stopper (depicted in the close-up view in Fig.1). Therefore, the length of *Sc* can be varied in the bending motion using the slider mechanism. The tips of these springs *Si*, *Sc*, and *So* are fixed to the rigid tip body (*Rt*). Ri_1, Ri_2, and Ri_3 are rigid prismatic bodies and are fixed to the center spring (*Sc*). The outer bodies Ro_1, Ro_2, and Ro_3 are hollow prismatic rigid bodies that allow the sliding motion of the inner rigid bodies and center spring in the long axis inside the bodies.

B. Motion

By applying a linear motion input to Ri_3 in the long axis toward the mechanism, the mechanism performs a bending motion (flexion), in rotating three joint parts (DIP, PIP and

MP) simultaneously. Fig.2 illustrates a time-series of pictures of the human finger bending motion of a healthy subject, the prototype mechanism, and the results of the FEM analysis. The details of the prototype design are described later in this section. Fig.3 illustrates the measured flexion and extension angles of the DIP, PIP, and MCP joints in unconstrained finger motion. For the measurement of the free mechanism motion, position control was performed with a repetitive back-and-forth motion at a constant velocity (10 s period within 11.6 mm of stroke length) on Ri_3 as the input linear motion. The angles were obtained using a motion analyzing microscope system (VW-6000, Keyence Co., Ltd. Japan). The motion was performed from the open position (finger and palm are straightened) to the flexed position (finger and thumb are opposed). In the free mechanism motion, a steep decrease of the angle at the MCP after 50 % of the movement cycle was observed due to the friction of internal mechanism, since the motion was unconstrained. However, these results showed that the mechanism and its analyzed motions were roughly in agreement with the human finger motion. A preliminary evaluation result is shown in Section III.B.

As described in Section I, configuring a mechanical RCM point to the center of the human joint is a challenge. In the proposed mechanism, three layers of springs, *Si*, *Sc*, and *So*, play a key role in performing the bending motion with the RCM in a simple and compact mechanism design. In each joint, the inner spring bends since both ends of the spring blade are fixed to rigid bodies during the bending motion. The center spring slides and bends simultaneously due to the linear motion input at the end of the mechanism. The outer spring also slides and bends due to the passive slider mechanisms integrated at the proximal end of each spring blade. These three-layered springs are then formed like a circular sector, providing an RCM at the center of the circular sector, as illustrated in Fig.4. By adjusting these RCM points to the human joints, the mechanism can properly guide and support natural human finger motion as a hand exoskeleton device. The stiffness of the three-layered springs plays a key role in the proper transmission of the bending motion from the proximal to the distal joints. In a compliant mechanism, the stress is concentrated at the point where the strength of the mechanical structure is relatively low; the deformation occurs at that point. Therefore, the stiffness of the springs at each joint must be designed properly to achieve a natural bending motion. The outer spring plays an important role in the transmission of the force to the distal joints by preventing excessive bending of the center spring. A more detailed discussion is provided in the evaluation section, Section III B. In this mechanism, both flexion and extension motion can be obtained by a pushing and pulling linear input motion. Note that the inner rigid bodies also prevent excessive bending (i.e., buckling). The outer rigid bodies are fixed to the finger to transmit force to guide or assist the finger motion. Note that the motion range of each joint can be limited by adjusting the stoppers on each passive slider mechanism on the outer spring (*So*) for safety. Also,

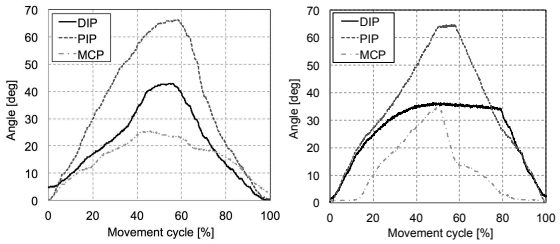

Fig. 3. Unconstrained flexion and extension movement of the human finger and the mechanism (left: human finger, right: proposed mechanism).

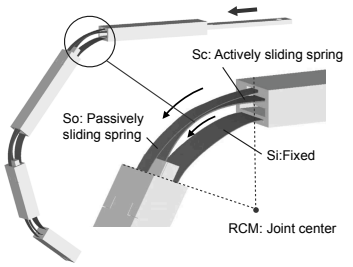

Fig. 4. Bending motion with RCM generated by the proposed three-layered sliding spring mechanism.

TABLE I

ANTHROPOMETRIC DATA OF A SUBJECT BASED ON WHICH THE PROTOTYPE DESIGNED IN THIS PAPER WAS DESIGNED.

Parameter	Value
$D_{DIP-PIP}$	23.0 [mm]
$D_{PIP-MCP}$	44.0 [mm]
T_{DIP}	11.3 [mm]
T_{PIP}	16.4 [mm]
T_{MCP}	26.5 [mm]

TABLE II

PROTOTYPE DESIGN PARAMETERS

Parameter / Parts	Value
To	1.7 [mm]
Ti	2.5 [mm]
Si_1	L:8.9, W:3.5, T:0.1 [mm]
Si_2	L:14.3, W:6.0, T:0.1 [mm]
Si_3	L:17.4, W:7.5, T:0.1 [mm]
Sc_1	L:12.8, W:2.0, T:0.2 [mm]
Sc_2	L:18.7, W:3.0, T:0.2 [mm]
Sc_3	L:20.6, W:4.0, T:0.2 [mm]
So_1	L:15.5, W:3.0, T:0.1 [mm]
So_2	L:21.7, W:3.0, T:0.1 [mm]
So_3	L:22.9, W:3.0, T:0.1 [mm]
Ro_1	L:17.2, W:9.0 [mm]
Ro_2	L:36.1, W:9.0 [mm]
Ri_1	L:17.2, W:6.5 [mm]
Ri_2	L:36.1, W:6.5 [mm]

L: length, W: width, T: thickness

the current mechanism design requires a personalized device to be fitted (i.e., different sizes and required output forces). The current mechanism structure only guides or supports the finger flexion/extension motion, i.e., it is not applicable to thumb adduction/abduction.

C. Design parameter definition and determination

In this mechanism, the human-finger-like bending motion can be obtained by adjusting the dimensions of the rigid bodies and the stiffness of the springs. These parameters are the key features of the mechanism. The size of the finger, range of motion, and joint stiffness of the person who

wears the device should be taken into account. The following parameters are required to be measured on each finger: the distance between the DIP and PIP joints ($D_{DIP-PIP}$), the distance between the PIP and MCP joints ($D_{PIP-MCP}$), and the thickness of the finger at the DIP joint (T_{DIP}), PIP joint (T_{PIP}), and MCP joint (T_{MCP}). We also determined the maximum angle of each joint that the device guides or supports as θ_{DIP}, θ_{PIP}, and θ_{MCP}. To and Ti (illustrated in Fig.1) are the perpendicular distances between the three-layered springs and can be determined mainly by general design requirements, such as size (generally, a thin structure is desired for the users). To and Ti also affect the magnitude of the output force on each joint since the three-layered sliding springs are used to transmit the torque to each joint. The width of the mechanism can also be determined by the design requirements. The lengths of the spring blades (LSi_1, LSi_2, LSi_3, LSc_1, LSc_2, LSc_3, $LSo1$, LSo_2, and LSo_3) and rigid bodies (LRt, LRo_1, LRo_2, LRo_3, LRi_1, LRi_2, and LRi_3) are strongly related to the motion of the mechanism. The lengths of the spring blades can be determined as the arc length of the circular sector composed of the spring blade and the RCM and are derived from the following equations:

$$LSi_1 = 2\,\pi\,\frac{H_{DIP}}{2}\,\frac{\theta_{DIP}}{360} \quad (1)$$

$$LSi_2 = 2\,\pi\,\frac{H_{PIP}}{2}\,\frac{\theta_{PIP}}{360} \quad (2)$$

$$LSi_3 = 2\,\pi\,\frac{H_{MCP}}{2}\,\frac{\theta_{MCP}}{360} \quad (3)$$

$$LSc_1 = 2\,\pi\,\frac{H_{DIP}+Hi}{2}\,\frac{\theta_{DIP}}{360} \quad (4)$$

$$LSc_2 = 2\,\pi\,\frac{H_{PIP}+Hi}{2}\,\frac{\theta_{PIP}}{360} \quad (5)$$

$$LSc_3 = 2\,\pi\,\frac{H_{MCP}+Hi}{2}\,\frac{\theta_{MCP}}{360} \quad (6)$$

$$LSo_1 = 2\,\pi\,\frac{H_{DIP}+Hi+Ho}{2}\,\frac{\theta_{DIP}}{360} \quad (7)$$

$$LSo_2 = 2\,\pi\,\frac{H_{PIP}+Hi+Ho}{2}\,\frac{\theta_{PIP}}{360} \quad (8)$$

$$LSo_3 = 2\,\pi\,\frac{H_{MCP}+Hi+Ho}{2}\,\frac{\theta_{MCP}}{360} \quad (9)$$

Then the length of the rigid bodies is determined as follows:

$$LRo_1 = D_{DIP-PIP} - \frac{1}{2}\left(\frac{LSi_1}{2}+\frac{LSi_2}{2}\right) \quad (10)$$

$$LRo_2 = D_{PIP-MCP} - \frac{1}{2}\left(\frac{LSi_2}{2}+\frac{LSi_3}{2}\right) \quad (11)$$

$$LRi_1 = LRo_1 \quad (12)$$

$$LRi_2 = LRo_2 \quad (13)$$

Note that the sum of the half spring lengths Si_1 and Si_2 were divided by two in Equations 10 and 11 to minimize the friction between the outer rigid bodies and the fingers due to the displacement of the rigid bodies according to the flexion and extension of the finger. LRt, LRo_3, and LRi_3 can be derived by the general design constraints (e.g., motor connections).

In addition to these parameters, the stiffness of the spring blades largely affects the motion. In this prototype, these were experimentally determined by repeated FEM analysis, as shown in the right column of Fig.2. In the FEM analysis, a linear motion on Ri_3 (with a repetitive back-and-forth

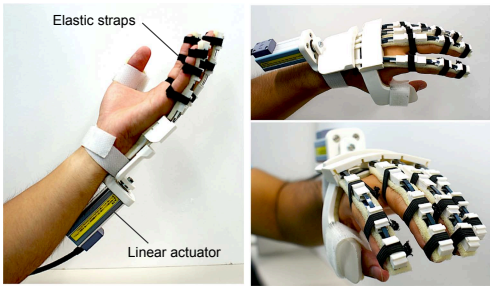

Fig. 5. Overview of the prototype.

motion at a constant velocity (10 s period with 11.6 mm of stroke length) was configured as a position input. The FEM analysis was conducted using the DAFUL mechanism analysis software (DAFUL Ver.3.3, Virtual Motion Inc.). We repeated the analysis varying the width and thickness of the spring blades until we obtained a desirable motion of the mechanism with reasonably manufacturable dimensions.

Finger grip forces during ADL have been identified to be around 10 N [21]. Therefore, the desired output force of the mechanism was set to 3 N for each of the four actuated fingers in this initial prototype. A hardened, cold rolled, special steel strip (JIS G3311, SK85M, Young's modulus: 210 GPa) was used as the spring material. This material was chosen due to its high elasticity. The rigid bodies were made of ABS resin using a rapid prototyping machine (uPrint SE Plus, Stratasys Ltd.).

The prototype described in this paper was designed based on the anthropometrics of a healthy subject (male, 27 years old, right handed). The parameters of the prototype are listed in Tables I and II. The first prototype was designed to guide or support the index finger motion from the open position (finger and palm are straightened) to the position where the index and thumb are opposed (depicted in the left column of Fig.2), taking into account the further utility of the device for rehabilitation.

III. Prototype Implementation and Evaluations

A. Prototype implementation

Based on the mechanism described in the previous section, we developed a prototype hand exoskeleton. An overview of the prototype is given in Fig. 5. The prototype consists of four finger modules: the index, middle, ring, and little fingers. In the prototype, the thumb is fixed at a predetermined angle in order to allow thumb opposition crucial for grasping function. The prototype can be fixed to the hand using an elastic strap on each part of the finger pad. All four actuated finger mechanisms are driven by a linear motor (RCA2-RP3N, IAI Corp. Co., Ltd.). Thereby, 12 flexion/extension joints are controlled using a single motor in the prototype. These 12 joints are not independently controlled, however, such a mechanically coupled DOFs with compliance provide natural synergistic movements of the device to achieve versatile grasping motions. The four finger mechanisms are fixed to the motor through a passive rotational joint on each finger; thus, passive adduction/abduction movements at the MCP joint can be performed. The weight of the prototype is 320

TABLE III

CHARACTERISTICS OF LINEAR MOTOR

Manufacturer	IAI Co., Ltd. Japan
Model	RCA2-RP3N-I-10-1-30-A1-N
Weight	240 [g]
Stroke	30 [mm]
Rated force	170.9 [N]
Repeated position accuracy	$\pm$ 0.02 [mm]
Max. speed	50 [mm/s]

g, including the motor (240 g). The technical characteristics of the linear motor are listed in Table III. The motor is controlled using Matlab xPC target, and the controller uses an EMG sensor (ID3PAD, Oisaka Co., Ltd. Japan). Therefore, the prototype system is capable of controlling the motion according to the signal obtained from the EMG sensor. The current control system implementation is preliminary; thus, the control scheme was equipped with simple PID control using the integrated EMG signal.

B. Preliminary evaluation

For preliminary evaluation of the developed prototype, we characterized the position and force output.

1) Motion control test: In this test, only the index finger module of the prototype was worn by a healthy subject (male, 27 years old, right handed, the same subject of design parameter definition). The subject was instructed to relax the finger, and the mechanism performed the motion from the original position (the index finger and palm are straightened) to the flexed position (the index and thumb are opposed). Fig.6 illustrates the prototype motion of the index finger in a series of pictures. Evolution of flexion/extension angles of each joint along the grasping movement cycle and the trajectory (MCP is located at the origin) are shown in Fig.7. To compare with the human natural bending motion, the bending motion without wearing the finger mechanism (upper) and wearing the finger mechanism (lower) were measured in the same experimental setup. The angles were obtained as described in section II.B. The observed maximum angles were 42.9 deg and 40.7 deg at the DIP, 66.3 deg and 67.3 deg at the PIP, 25.5 deg and 36.7 deg at the MCP, on the human finger and the prototype worn by a subject, respectively. These maximum angles were observed in the motion cycle of 54.4 % and 53.6 % at the DIP, 66.3 % and 67.3 % at the PIP, and 25.5 % and 36.7 % at the MCP. The difference of the maximum angle (11.2 deg) and peak position in the motion cycle (13.9 %) was observed at the MCP, due to the mechanical constraint on the thumb. However, the results show that the mechanically guided motion of the prototype corresponded well to the natural finger motion. From the series of pictures (Fig.6), it was seen that the prototype could smoothly guide the subject's index finger to perform the motion. The compliance of the mechanism was considered to be the main reason for such natural finger-like motion since the mechanism inherently has an elastic structure that can adjust to the finger motion. The hysteresis observed in the unconstrained motion (illustrated in the right panel of Fig.3) was not observed in the result. This can be

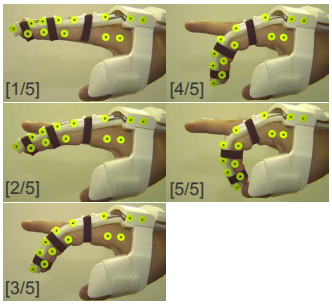

Fig. 6. Time series of pictures of the prototype in motion (only the index finger for measurement)

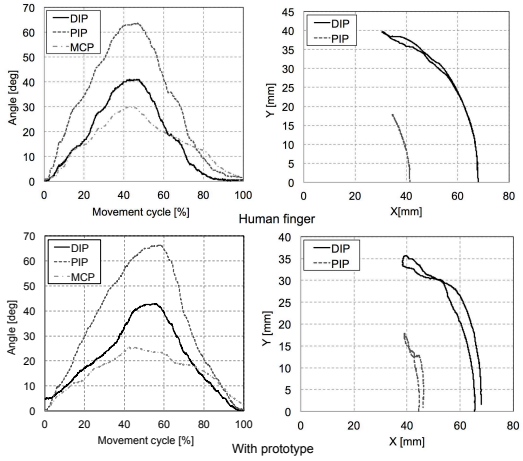

Fig. 7. Position measurement results for finger motion (upper: human finger, lower: prototype worn by a subject)

explained by to the mechanical guidance from the human hand. However, further evaluation and analysis are required to further investigate this property.

2) Output force measurement: To evaluate the output force that the device can exert on the finger, we tested the finger module motion under load. In the test, a weight of 300 g was attached to each of the outer rigid bodies, and finger flexion/extension motion was performed.

The motion was successfully performed in all of the test conditions. As a representative result, a series of pictures are shown in Fig.8 (flexion: the load was applied to Ro_t). In the pictures in Fig.8, the motion of the finger was significantly distorted due to the load applied; however, this was not observed in the preliminary test on the subjects since the mechanism can be properly guided by the subject's finger. To quantitatively assess the output force, we are currently preparing a dummy finger rig with force sensors in all of the joints that will allow us to precisely measure the output force. In addition, FEM analysis with a payload on each joint in various conditions is underway.

As described in Section II B, the stiffness of the springs is strongly related to the magnitude of the maximum force. In addition, it was shown in preliminary FEM analysis that the outer spring plays an important role in the transmission of the force to the distal joints by preventing excessive bending of the center spring. In this prototype, these parameters were experimentally determined by repeated FEM analysis.

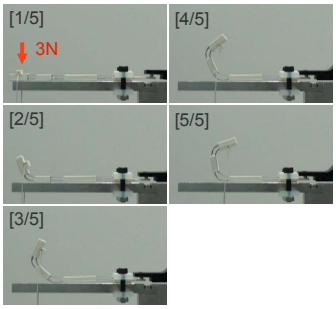

Fig. 8. Time series of pictures of representative behavior in output force measurement. The motion was performed by attaching a load of 3 N at Ro_t.

However, a more detailed kinematic model including such characteristics of a compliant structure will be required for further optimization.

IV. Conclusions

In this paper, a three-layered sliding spring mechanism was proposed to be applied to a hand exoskeleton device. In the proposed mechanism, the elastic components are serially connected to perform the flexion/extension of three joints by a single actuator as an under-actuated mechanism. The advantage of the mechanism is that it is compact and lightweight, and most importantly, since the mechanism involves compliant elements, the device can be inherently compliant for safety. In addition, the proposed mechanism adequately distributes 1-DOF actuated linear motion into 3-DOF rotational motions of finger joint (DIP, PIP, and MCP) to realize a natural finger flexion/extension. Such mechanical flexibility can also be useful to provide a high adaptability to complex objects in ADL.

From a mechanical point of view, the most interesting feature of the proposed mechanism is the serially connected compliant elements, which consist of mechanical chains on elements with layered springs. The prototype of the hand exoskeleton using the proposed mechanism showed that the device provides biomechanically correct motion, and can potentially be effective for supporting activities of daily living.

However, a more detailed modeling of the mechanism is required for further investigation and optimization. An Analysis and evaluation on the motion hysteresis is one of the issues to be addressed in future work. We are currently working on further optimization of the kinematics using both FEM analysis and prototype experiments.

The prototype presented in this paper has been tested on different adult subjects (average-sized males and females). We initially assumed that a personalized design would be required for each hand size; however, the prototype clearly showed good fitting with different hand sizes. Therefore, the mechanism might not need precise personalization. This could be because the compliant mechanism structure and elastic straps function as inherent alignments. We are currently evaluating the size adjustment issue in a wider range of subjects. We aim to test this device in patients, and to eventually also develop a version for home use to provide assistance/therapy in activities of daily living.

References

[1] S. Balasubramanian, J. Klein, E. Burdet, "Robot-assisted rehabilitation of hand function," Current Opinion in Neurology, vol.23(6), pp.661-670, 2010.

[2] H. I. Krebs, N. Hogan, M. L. Aisen and B. T. Volpe, "Robot-Aided Neurorehabilitation," IEEE Trans on Rehabilitation Engineering, vol.6(1), pp.75-87, 1998.

[3] W. S. Harwin, J. L. Patton, V. R. Edgerton, "Challenges and Opportunities for Robot-Mediated Neurorehabilitation," Proceedings of the IEEE, vol.94(9), pp.1717-1726, 2006.

[4] P. Raghavan, "The Nature of Hand Motor Impairment After Stroke and Its Treatment," Current Treatment Options in Cardiovascular Medicine, Vol.9, pp.221-228, 2007.

[5] O. Lambercy, L. Dovat, H. Yun, S. K. Wee, C. Kuah, K. S. G. Chua, R. Gassert, T. Milner, C. L. Teo and E. Burdet, "Effects of a robot-assisted training of grasp and pronation/supination in chronic stroke: a pilot study," Journal of NeuroEngineering and Rehabilitation, 8(63), 2011.

[6] K. Y. Tong, S. K. Ho, P. M. K. Pang, X. L. Hu, W. K. Tam, K. L. Fung, X. J. Wei, P. N. Chen, M. Chen, "An Intention Driven Hand Functions Task Training Robotic System," Proc. of Int. Conf. IEEE Engineering in Medicine and Biology Society, pp.3406-3409, 2010.

[7] B. L. Shields, J. A. Main, S. W. Peterson, A. M. Strauss, "An Anthopomorphic Hand Exoskeleton to Prevent Astronaut Hand Fatigue During Extravehicular Activities," IEEE Transactions on Systems, Man, and Cybernetics Part A: Systems and Humans, 27(5), pp.668-673, 1997.

[8] B. H. Choi, H. R. Choi "SKK Hand Master -Hand Exoskeleton Deriven by Ultrasonic Motors," Proc. of IEEE/RSJ Int. Conf. on Intelligent Robots and Systems, pp.1131-1136, 2000.

[9] S. Ito, H. Kawasaki, Y. Ishigure, M. Natsume, T. Mouri, Y. Nishimoto, "A design of fine motion assist equipment for disabled hand in robotic rehabilitation system," Journal of the Franklin Institute, vol.348(1), pp.79-89, 2011.

[10] S. Sugano, S. Tsuto and I. Kato, "Force Control of the Robot Finger Joint equipped with Mechanical Compliance Adjuster," Proc. of IEEE/RSJ Int. Conf. on Intelligent Robots and Systems, pp.2005-2013, 1992.

[11] M. Turner, D. Gomez, M. Tremblay, and M. Cutkosky, "Preliminary tests of an arm-grounded haptic feedback device in telemanipulation," Proc. of ASME WAM, DSC-64, pp.145-149, 1998.

[12] T. T. Worsnopp, M. A. Peshkin, J. E. Colgate, and D. G. Kamper, "An Actuated Finger Exoskeleton for Hand Rehabilitation Following Stroke," IEEE 10th International Conference on Rehabilitation Robotics, pp.896-901, 2007.

[13] J. Wang, J. Li, Y. Zhang, S. Wang, "Design of an Exoskeleton for Index Finger Rehabilitation," Proc. Conf. of the IEEE Engineering in Medicine and Biology Society, pp.5957-5960, 2009.

[14] Y. Hasegawa, Y. Mikami, K. Watanabe and Y. Sankai, "Five-Fingered Assistive Hand with Mechanical Compliance of Human Finger," Proc. of IEEE Int. Conf. on Robotics and Automation, pp.718-724, 2008.

[15] H. Yamaura, K. Matsushita, R. Kato and H. Yokoi, "Development of Hand Rehabilitation System for Paralysis Patient - Universal Design using Wire-Driven Mechanism -," Proc. Conf. of the IEEE Engineering in Medicine and Biology Society, pp.7122-7125, 2009.

[16] D. G. Caldwell, O. Kocak and U. Andersen, "Multi-armed Dexterous Manipulator Operation using Glove/Exoskeleton Control and Sensory Feedback," Proc. of IEEE/RSJ Int. Conf. on Intelligent Robots and Systems, pp.567-572, 1995.

[17] M. Bouzit, G. Burdea, G. Popescu and R. Boian, "The Rutgers Master II - New Design Force-Feedback Glove," IEEE/ASME Trans. on Mechatronics, vol.7(2), pp.256-263, 2002.

[18] L. Connelly, Y. Jia, M. L. Toro, M. E. Stoykov, R. V. Kenyon and D. G. Kamper, "A Pneumatic Glove and Immersive Virtual Reality Environment for Hand Rehabilitative Training After Stroke," IEEE Trans. on Neural Systems and Rehabilitation Engineering, vol.18(5), pp.551-559, 2010.

[19] L. L. Howell, *Compliant mechanisms*, Wiley-Interscience, ISBN 978-0-471-38478-6, 2001.

[20] N. Lobontiu, *Compliant mechanisms*, CRC Press, ISBN 978-0-8493-1367-7, 2002.

[21] N. Smaby, M. E. Johanson, B. Baker, D. E. Kenney, W. M. Murray, V. R. Hentz, "Identification of key pinch forces required to complete functional tasks," J Rehabilitation Research & Development, Vol.41(2), pp.215-224, 2004.